1   **Starch degradation and intermediate dynamics in flocculated and dispersed**

2   **microcosms**

3

4   Kristin T. Ravndal* and Roald Kommedal

5   University of Stavanger, Department of Mathematics and Natural Science, 4036

6   Stavanger, Norway

7

8   * Corresponding author: Kristin T. Ravndal, Current address: Cranfield Water Science

9   Institute, Cranfield University, Bedfordshire, MK43 0AL, UK, e-mail:

10   kristin.t.ravndal@cranfield.ac.uk

11   Co-author e-mail: roald.kommedal@uis.no

12

Abstract

A large fraction of the organic substrate in municipal wastewater is particulate. Prior to uptake, particles have to be degraded through potentially a range of intermediates. However, research on intermediate dynamics during particle hydrolysis is limited. In this paper batch experiments on flocculated and dispersed biomass microcosms using starch as particulate substrate are reported. Overall hydrolysis rate was not significantly different between the two systems. Particle colonization, increased particle porosity in combination with particle breakup led to increased substrate availability over time. Particle breakup was more important for flocculated biomass, while increased particle porosity and particle colonization played a larger role for dispersed biomass. During particle degradation intermediates were formed, however, all intermediate polymer sizes were not formed to the same extent. This can be explained by non-random enzymatic degradation, where some products are preferred over others. Intermediates dynamics also depend on the biomass structure, and in a floc based system, diffusion limitations allow glucose to accumulate in the system.

Keywords

Particle colonization

Particle breakup

Intermediate dynamics

Hydrolysis

Starch

Abbreviations

DRI: differential refractive index detector

F/M-ratio: Food to mass ratio

HMW: High molecular weight

LMW: Low molecular weight

MALS: Multi angle light scattering detector

MMW: Medium molecular weight

OUR: Oxygen utilization rate

PBM: Particle break-up model

PSD: Particle size distribution

SEC: Size exclusion chromatography

SPM: shrinking particle model

ThOD: Theoretical oxygen demand

Introduction

Municipal wastewater consist of a large fraction of particulate organic matter (41-73 %; Levine et al. 1991), hence, particle degradation dynamics is important for process analysis in wastewater treatment. In general, particles cannot be directly taken up by bacterial cells, but has to undergo extracellular depolymerisation until molecules small enough for transport across the bacterial cell membrane are available. Size limit for cellular uptake is generally assumed to be 0.6-1 kDa (White et al. 2012). Hydrolytic and lytic depolymerisation are the dominant mechanisms of depolymerisation, and theoretically allow for any sub-polymeric intermediate to be formed. Most work on depolymerisation dynamics focus on easily biodegradable substrate formation kinetics, while research on intermediate dynamics during particle hydrolysis is limited.

Starch is a common model substrate for slowly biodegradable substrate in wastewater (Karahan et al. 2006). Being a natural constituent in municipal wastewater, starch-hydrolysing organisms are abundant in activated sludge (Xia et al. 2008). Starch is also a common biodegradable particle in industrial wastewater from the textile industry (Feitkenhauer & Meyer 2002), in addition to food processing industrial wastewaters. Native starch from various plant sources are composed of the α1,4-linked glucosidic polymers amylose and amylopectin (Ball et al. 1996; Dona et al. 2010; Oates 1997). Amylopectin is the major component of starch, a highly α1,6-branched water-soluble polymer with a molecular weight of 10^4-10^6 kDa (Ball et al. 1996; Dona et al. 2010). Amylose is a smaller linear insoluble polymer of molecular weight range 100-1000 kDa (Ball et al. 1996).

71   Different mechanisms and modelling approaches have been proposed for particle

72   hydrolysis (Morgenroth et al. 2002; Vavilin et al. 2008). In a model for anaerobic

73   digestion proposed by Vavilin et al. (1996) solid waste particles are assumed to be

74   colonized by hydrolytic bacteria, who subsequently produce hydrolytic enzymes.

75   Colonization (biofilm growth covering the particle surface) was in a previous study

76   observed by microscopy and proposed as the main mechanism for particle degradation

77   in a biologically activated membrane bioreactor (Ravndal et al. 2015). In activated

78   sludge processes, bacteria grow in flocs and the initial step of starch degradation has

79   been proposed as adsorption of starch to the flocs (Ciggin et al. 2013; Karahan et al.

80   2006; Martins et al. 2011).

81   Regardless of whether degradation of particulates work through colonialization or flocs

82   adsorption, degradation will depend on available particle surface area. In addition to the

83   particle – biomass contact perspective, particle degradation also depends on the particle

84   morphology. Two different models proposed are the shrinking particle model (SPM;

85   Sanders et al. 2000) and the particle breakup model (PBM; Dimock & Morgenroth

86   2006). The SPM assumes particles to shrink gradually as they are degraded, hence

87   available surface area decrease. In the PBM, particles break up as they are degraded

88   leading to an increase in available surface area. Hence, in the PBM, surface area to

89   volume ratio are included as a state variable in the model. An open question of the PBM

90   is whether the kinetics observed also could be caused by increased particle porosity

91   leading to increased surface area to volume ratio or increased particle colonization

92   (Dimock & Morgenroth 2006).

93   The hydrolysis process is an enzymatic degradation process as discussed in both the

94   activated sludge models (Henze et al. 2000) and anaerobic digestion model (Batstone et

al. 2002). Hydrolytic enzyme kinetics are independent of electron acceptor conditions (Goel et al. 1998), hence hydrolysis studied under aerobic conditions is also relevant for anaerobic conditions and vice versa. The concentration of hydrolytic enzymes, however, may depend on electron acceptor conditions (lower concentrations under anaerobic conditions) probably due to correlation to cellular yield (Kommedal 2003). For starch degradation, a range of extracellular enzymes are active (Robyt 2009), and a substantial collection of published articles on characteristics of starch degrading enzymes is available (Sun et al. 2010). However, less attention has been granted the combined substrate and biomass effect, and their influence on the substrate degradation dynamics.

In this study we address the need for more detailed knowledge of particulate organic matter degradation by (i) investigating starch particle degradation and intermediate dynamics including the entire size range from micrometer scale particles, polymers, oligomers and monomers (substrate size intermediate dynamics), and (ii) evaluate whether there is a difference in particle and intermediate dynamics for biomass aggregates or dispersed biomass (the substrate - biomass size effects). Our hypothesis is that 1) Starch is degraded via potentially all intermediate size ranges and that the kinetics is size dependant; and 2) Intermediate dynamics depends on the biomass structure, especially during the particulate substrate phase.

Materials and Methods

Batch experiments with starch as sole substrate, inoculated with activated sludge and dispersed activated sludge were analysed over a period of 117 days. Oxygen utilisation rate (OUR) was monitored, and sampling was performed regularly for particle size distribution (PSD) and polymeric, oligomeric and monomeric intermediates formation.

118 Particle morphology and particle – biomass interaction were observed by light

119 microscopy. Polymeric intermediate dynamics was followed using SEC in combination

120 with multi angle light scattering detector (MALS) and differential refractive index

121 detector (DRI), a technique with absolute determination of molar mass and mass

122 concentration, allowing for molecular mass determination without using molecular

123 standards (Cheong et al. 2015; Wyatt 1993).

124 Experimental setup

125 Batch tests were prepared at an initial volume of 500 mL and concentration of 2.00 g L^{-1}

126 of potato starch (Fluka Analytical 03967) in tap water. An initial high food to mass ratio

127 (F/M-ratio) was chosen in order to emphasize the substrate size effects (comparably low

128 initial biomass concentration). Inorganic nutrients were added (at concentrations 32.4

129 mg L^{-1} K_2HPO_4, 1.6 mg L^{-1} KH_2PO_4, 50 mg L^{-1} $NaNO_3$, 1.2 mg L^{-1} NH_4Cl, 0.1 mg L^{-1}

130 $FeCl_3$, 5 mg L^{-1} $CaCl_2$ and 3 mg L^{-1} $MgSO_4$) in addition to trace elements according to

131 Balch et al. (1979). Amino acids (10 µL, R 7131 RPMI-1640 [50X], Sigma Aldrich)

132 and vitamins (10 µL, B6891 BME [100X], Sigma Aldrich) were also added to each test

133 bottle. Test bottles (five replicates) were inoculated with 500 µL activated sludge or 500

134 µL dispersed activated sludge (four replicates). Activated sludge was collected at Vik

135 wastewater treatment plant (Rogaland, Norway), from the aerated bioreactor containing

136 approximately 4 g L^{-1} mixed liquor suspended solids, giving an estimated initial

137 suspended total solids concentration in test bottles of 2.5 mg TSS L^{-1} (F/M-ratio >

138 1000). Dispersed activated sludge was prepared by sonication (Branson 2510 Sonicator,

139 100W) of a sub-volume of collected sludge for a total of 20 min in 5 min intervals to

140 minimise temperature increase. Sonication efficiency was confirmed by microscopy,

141 and positive controls inoculated with glucose was used to validate viability of sonicated

142   cells. Sampling for particle and intermediate analysis was performed by drawing 5 mL

143   samples from the batch tests throughout the experiment every 3-7 days until day 62,

144   every 12-14 day until day 88 and a last sampling at day 117.

145   ## Oxygen utilization rate

146   OUR was monitored on-line by a Micro-oxymax dynamic respirometer (Columbus

147   Instruments, Ohio, USA) measuring oxygen concentration in the gas phase of each test

148   bottle (653 mL) 21.6 times per day. The respirometer was equipped with a paramagnetic

149   oxygen sensor (Paramax-101, Columbus Instruments, Ohio, USA). To ensure aerobic

150   conditions, the respirometer refreshed the gas phase when the O_2 concentration fell

151   below 18.9 mole %.

152   ## Particle size measurements

153   PSDs were analysed by a Multisizer 4 coulter counter (Beckman Coulter) using 0.9 M%

154   NaCl as electrolyte. Samples were vortexed before diluting 1-2.5 mL of the sample to

155   200 mL with 0.9 M% NaCl. Analysis was performed with a 200 µm aperture tube

156   (measurement range 4-120 µm) in volumetric mode analysing 2 mL of the diluted

157   sample. Electrolyte blanks were analysed for subtraction of background noise.

158   ## Light microscopy

159   A qualitative observation of particles and biomass in the batch tests was performed

160   using light microscopy (Olympus BX61 microscope, 100x oil Plan Fluorite objective

161   with iris) equipped with a CCD camera (Olympus DP72). Image acquisition and

162   analysis was performed using cellSens Dimension 1.3 software (Olympus).

Polymer analysis

SEC in connection with MALS and DRI detectors was used to separate and analyse intermediates in the polymeric range of 1-10^6 kDa. An Agilent 1260 Infinity HPLC system with a quaternary pump was equipped with a PL-aquagel-OH50 (Agilent) and a PL-aquagel-OH30 (Agilent) column in series. Sodium nitrate (50 mM) was filtered with 0.1 µm cellulose nitrate membrane filters (Whatman) and used as mobile phase. Two detectors were connected to the system in series, a MALS detector (Dawn 8^+, Wyatt Technology) and a DRI detector (Optilab T-rEX, Wyatt Technology). Flowrate during analysis was 0.75 mL min^{-1} and the column was kept at 30 °C by a column oven (Agilent 1260 column compartment). All samples were filtered through 0.45 µm Marcherey-Nagel Nanocolor 50 chromafil GF/PET membrane filters prewashed with deionized water. 100 µL sample was injected. Two parallel samples were withdrawn from all bottles at each sampling time, one sample was filtered, while the other was filtered and heated to 85 °C for 5 min to denature extracellular enzymes. Resulting mass and molar mass of the two samples were compared, and found to be comparable between samples. The universal refractive index increment (dn/dc) value of 0.15 for polysaccharides in water with low salt concentration was used (Cheong et al. 2015). Based on the chromatograms polymers were separated in three size fractions, low molecular weight (LMW), medium molecular weight (MMW) and high molecular weight (HMW). Molecular weight of HMW fraction was measured by the MALS detector. LMW and MMW fractions had a low light scattering signal, and molecular weight was estimated based on dextran calibration standards. LMW polymers were in the size range from 1-12 kDa, and MMW polymers in the range from 12-350 kDa.

Monomer and oligomer analysis

Concentrations of glucose, maltose, isomaltotriose, maltotetraose and maltopentaose in
the bulk liquid was measured using an Agilent 1100 series HPLC system with a
quaternary pump connected to an ELSD-detector (3300 ELSD, Alltech). The system
was equipped with a Shodex combined SEC and ion-exchange column (Sugar KS-802,
Showa Denko Europe GmbH). Mobile phase was Milli-Q quality water at a flow rate of
0.75 mL min^{-1}. Column temperature was kept at 80 °C using a column oven (Eppendorf
CH-30). The ELSD detector had a N_2-gas flow of 1.3 L min^{-1} and held a temperature of
35 °C, gain was set at 16. Calibration standards used were D(+)-glucose (Merck), D-
(+)-maltose monohydrate from potato (Sigma Aldrich M5885), isomaltotriose (Sigma
M8378), maltotetraose (Supelco 47877), and maltopentaose (Supelco 47876).

Results

Oxygen utilization rate

OUR (figure 1) was monitored in five parallel batch tests inoculated with flocculated
biomass, and four parallel batch tests inoculated with dispersed biomass. OUR trends
were similar for flocculated and dispersed biomass tests. An initial fast increase in rate
was observed between day 2 and 4. Between day 4 and 36 OUR was stable at 2.0 ± 0.4
mg L^{-1} h^{-1} and 1.8 ± 0.4 mg L^{-1} h^{-1} for flocculated and dispersed biomass batch tests,
respectively. A steady decrease in OUR was observed after 36 days, before the rate
stabilized at a low level after 87 and 78 days for respectively flocculated and dispersed
biomass tests. After 97 days, accumulated oxygen consumption was 2978 ± 116 mg L^{-1}
for flocculated biomass and 2451 ± 102 mg L^{-1} for dispersed biomass. Based on initial
starch concentration, theoretical oxygen demand (ThOD) was 2380 mg L^{-1}, within the

209 range for the dispersed biomass, but lower than measured accumulated oxygen

210 consumption for the flocculated biomass. The overestimation was due to large batch test

211 variability and single batch instrumental errors during the experiment.
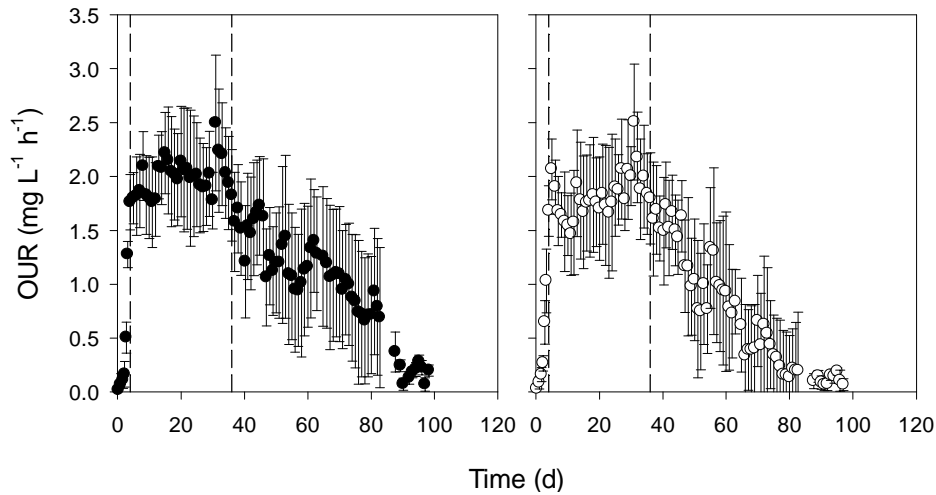
212

213 **Figure 1:** OUR in ● activated sludge and ○ dispersed activated sludge batch tests. Dashed lines indicate

214 a shift in OUR trend at 4 and 36 days. Error bars indicate standard error.

215

Particle dynamics

217 Total particle number, volume and surface area were measured in all batch tests, and

218 surface area to volume ratio was calculated (figure 2). Surface area to volume ratio

219 increased before stabilizing after 32 days at 0.58 ± 0.06 µm^{-1} and 0.56 ± 0.06 µm^{-1} for

220 flocculated and dispersed biomass tests, respectively. This corresponds to a mean

221 spherical particle diameter of 10 µm. Total particle number, volume and surface area all

222 had an early stage increase before a maximum was reached after 20 d, 6 d and 20 d,

223 respectively, for both flocculated and dispersed biomass batch tests. After the early

224 increase, all three variables decreased and reached a stable level after 44 days. Particle

11

225 number became constant at a higher level than the initial value, while particle volume

226 and surface area arrived at lower than initial values. Change in PSD was monitored as a

227 function of time (figure 3). Initially most of the particle volume detected was distributed

228 between 10 µm and 70 µm. with a peak at 35 µm. Distribution shifted towards smaller

229 particle sizes over time, and after 20 days peak maxima was at a particle diameter of 12

230 µm and 18 µm for flocculated and dispersed biomass tests, respectively. Flocculated

231 biomass batch tests had an overall higher particle volume than dispersed biomass tests.
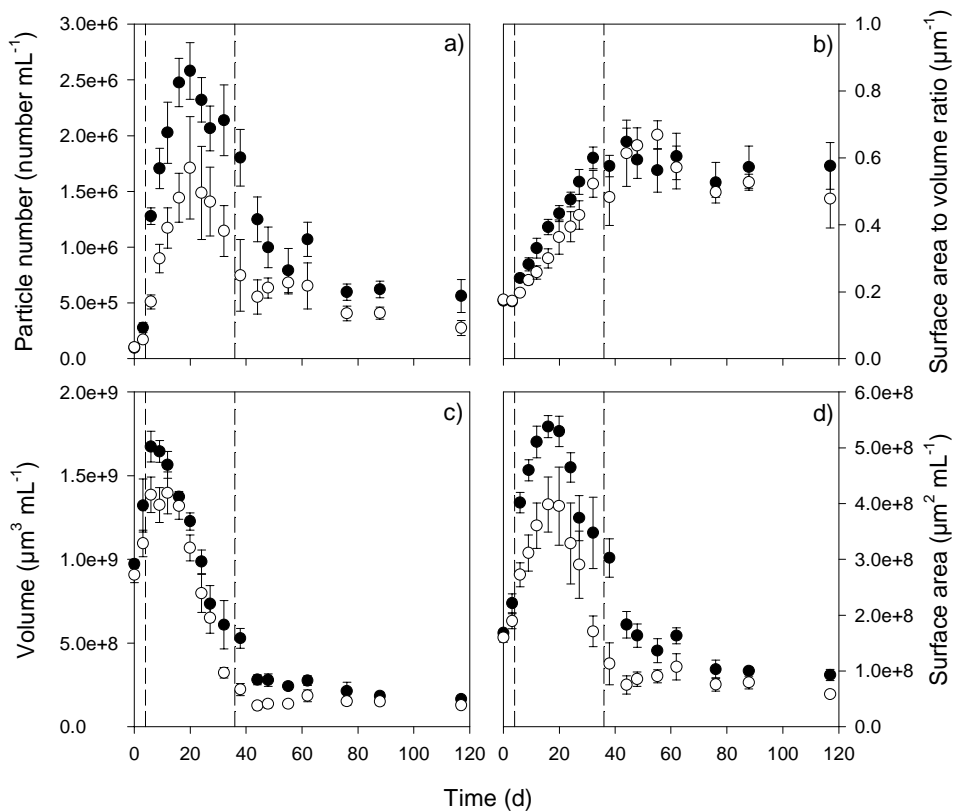
232

233 **Figure 2:** a) particle number (number mL^{-1}), b) surface area to volume ratio (µm^{-1}), c) particle volume

234 (µm^3 mL^{-1}), d) particle surface area (µm^2 mL^{-1}) measured over 117 days in ● activated sludge and ○

235 dispersed activated sludge batch tests. Dashed lines indicate a phase shift at day 4 and day 36. Error bars

236 indicate standard error.

237
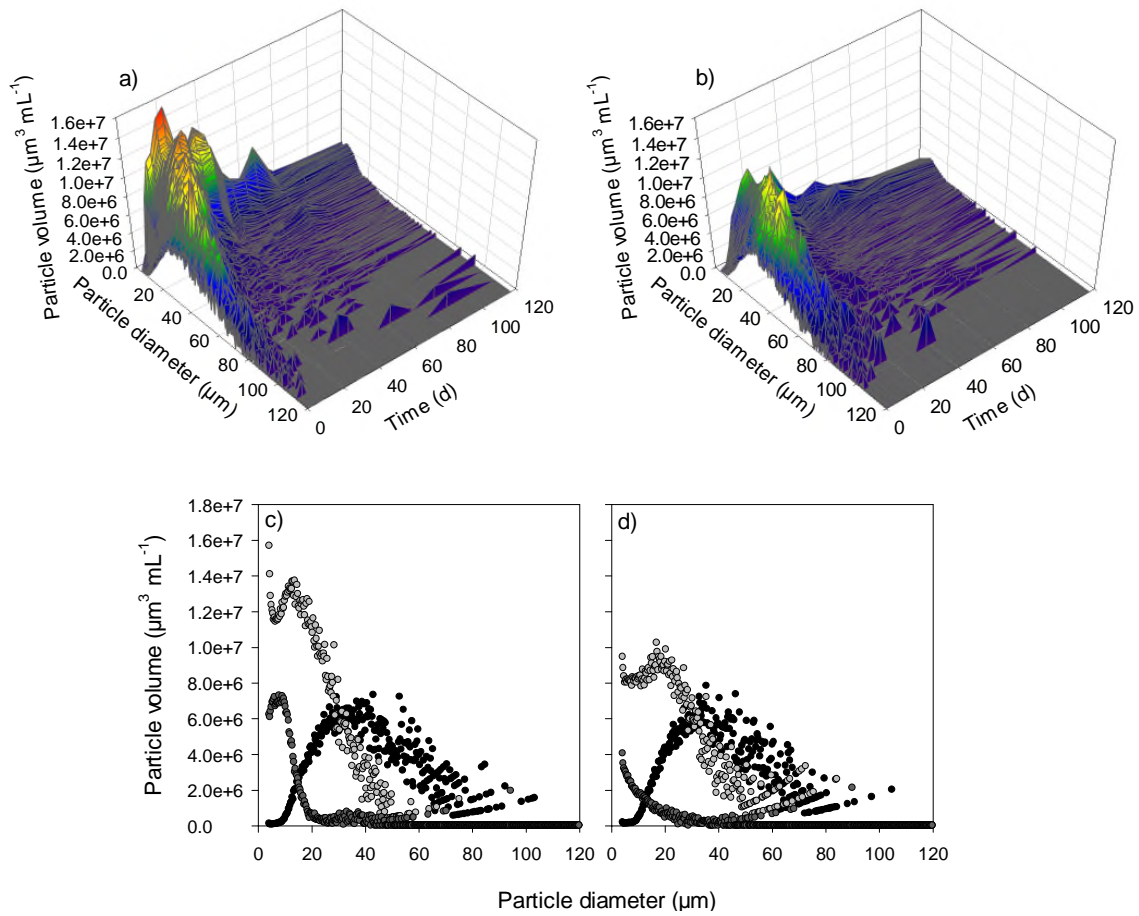
Figure 3: Change in PSD over time in a) activated sludge batch tests and b) dispersed activated sludge

batch tests, and PSD at ● day 0, ● day 20, ● day 44 in c) activated sludge batch tests and d) dispersed

activated sludge batch tests.

Brightfield microscopy images were collected for flocculated and dispersed biomass

batch tests (figure 4). Due to the high F/M-ratio chosen, at day 0 mainly starch particles

were observed. Starch particles colonized by microbial biomass was observed at day 3,

and over time the particle surface cracked and particles broke up. After 38 days only

microbial biomass was observed. Images from flocculated and dispersed biomass tests

were similar, particle colonization, particle cracking and particle breakup was observed

in both types of tests.

249
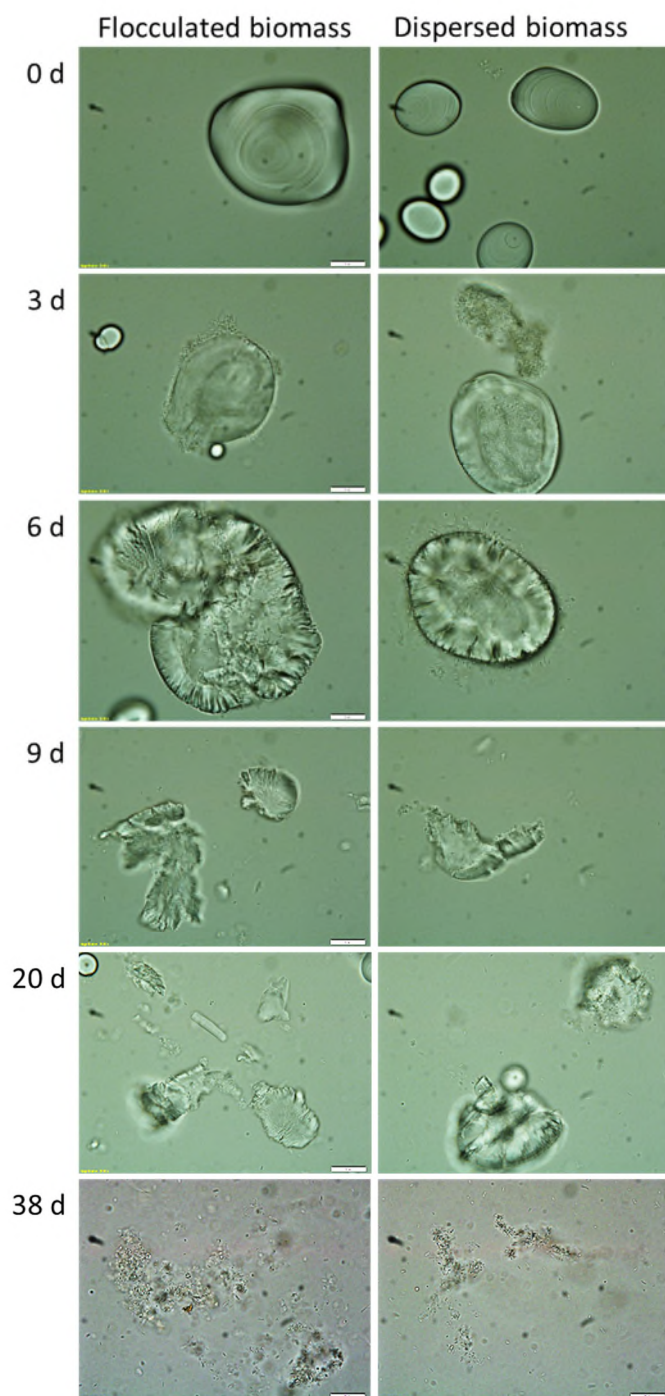
Figure 4: Brightfield microscopy images at 0, 3, 6, 9, 20 and 38 days for flocculated and dispersed

biomass batch tests. Bar length is 20 µm. Picture at day 0 show smooth starch particles, day 3 show

colonized starch particles (microbial biomass covering the surface of the starch particle), day 6 cracked

254 and colonized starch particles, day 9 and 20 show starch particles that have been broken up, and day 38

255 show microbial biomass.

Intermediate dynamics

257 Monomer, oligomer and polymer intermediates were measured in the bulk liquid of

258 batch tests inoculated with flocculated and dispersed biomass (figure 5). When

259 flocculated biomass was used as inoculum, glucose was detected in the bulk liquid the

260 first two weeks of the experiment with a maximum measured concentration of 54 ± 21

261 mg L^{-1}. Glucose was not detected above 2 mg L^{-1} in dispersed biomass tests. Maltose

262 was measured between day 3 and 20 at a maximum concentration of 28 ± 14 mg L^{-1} and

263 36 ± 31 mg L^{-1}, respectively, in flocculated and dispersed biomass tests. Isomaltose,

264 maltotetraose and maltopentaose were detected at low levels in both flocculated and

265 dispersed biomass tests between day 3 and 20. LMW polymers were present at a

266 background level of about 20 mg L^{-1} at the start of the experiment. Concentration of

267 LMW polymers increased after day 3, reached a maximum of 142 ± 23 mg L^{-1} after 12

268 days for flocculated biomass and 125-130 mg L^{-1} between day 9 and 20 for dispersed

269 biomass. After peak concentrations, a gradual decrease back to the background level

270 after 60 days was observed. Concentration of MMW polymers in the bulk liquid

271 increased between day 32 and 76, with maximum peak concentration of less than 20 mg

272 L^{-1} at day 48 for flocculated biomass and day 55 for dispersed biomass batch systems.

273 HMW polymers were detected in the bulk liquid from day 9 to 88 with a maximum

274 concentration of 70 ± 13 mg L^{-1} after 48 days for flocculated and 48 ± 8 mg L^{-1} at 55

275 days for dispersed biomass. In the period between day 6 to 88, average molecular

276 weight of the HMW polymer fraction was 8222 ± 1210 kDa and 9496 ± 1408 kDa for

277 flocculated and dispersed biomass tests, respectively (figure 6). Molecular weight in

278   flocculated biomass batch tests had an early increase with a peak at 12 days, before

279   steadily decreasing until the end of the experiment. Dispersed biomass tests had the

280   same early increase, but did not show the same decrease towards the end of the

281   experiment.

282
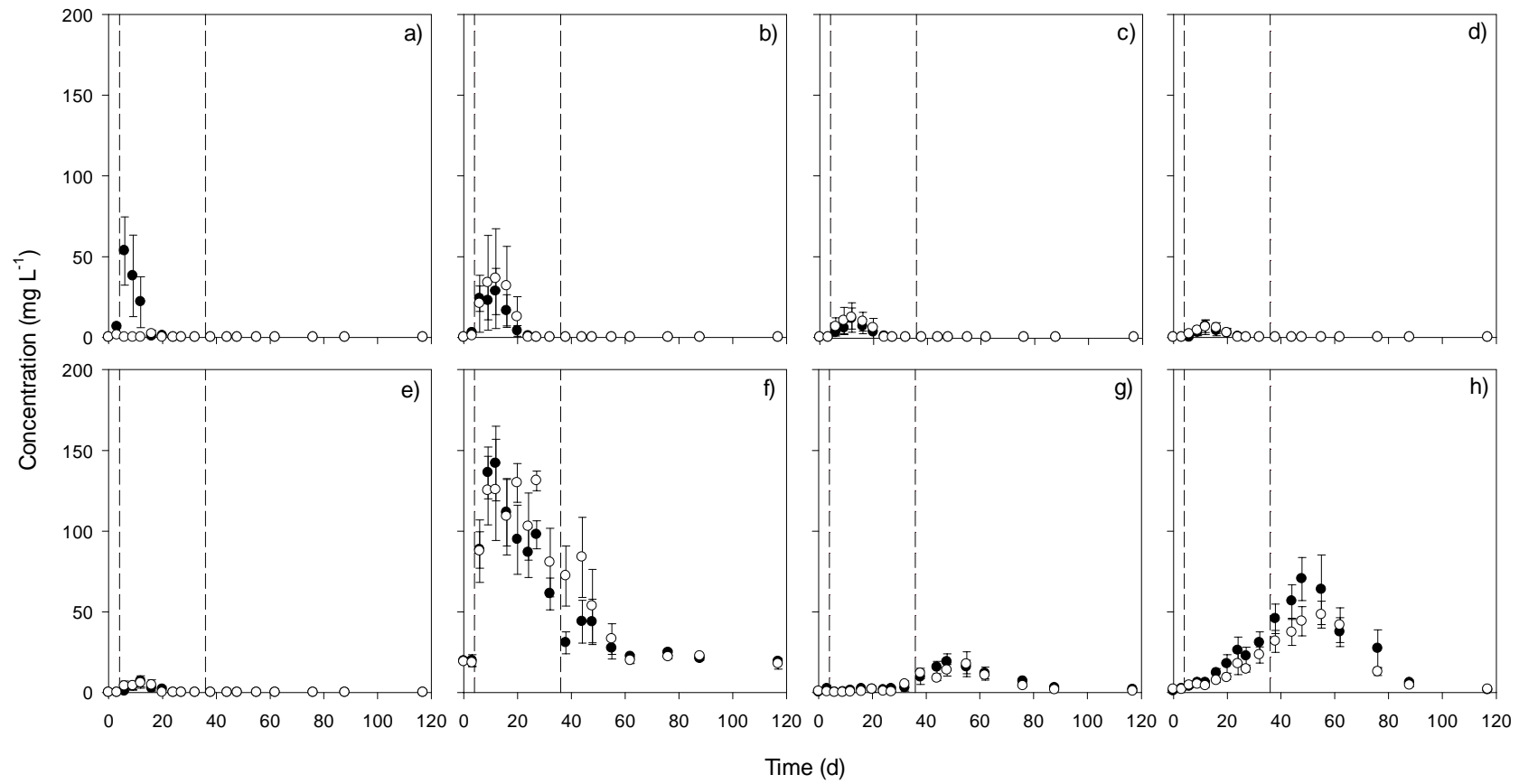
Figure 5: Concentration (mg L-1) of a) glucose, b) maltose, c) isomaltotriose, d) maltotetraose, e) maltopentaose, f) LMW polymers, g) MMW polymers and h) HMW polymers in ● activated sludge and ○ dispersed activated sludge batch tests. Dashed lines indicate a phase shift at day 4 and day 36. Error bars indicate standard error.
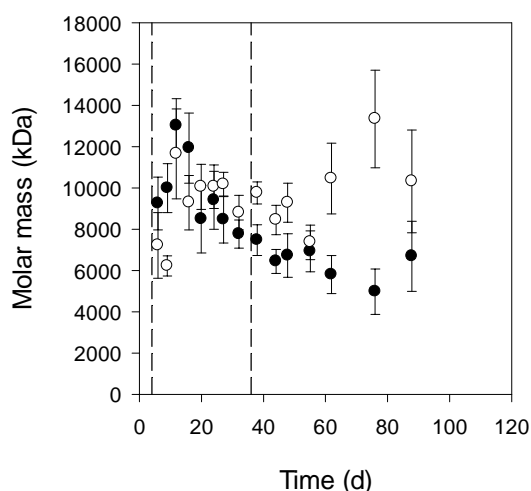
Figure 6: Molar mass (kDa) of polymeric fraction in ● activated sludge and ○ dispersed activated sludge batch tests. Dashed lines indicate a phase shift at day 4 and day 36. Error bars indicate standard error.

Discussion

Starch degradation in batch experiments

Starch particles and microbial biomass are both particulate and will not be distinguished by coulter counter analysis. In the first days, total particle volume increased (figure 2), likely due to microbial biomass growth and starch granule swelling. Swelling was also observed by microscopy showing larger and more heterogeneous starch particles after 3-6 days. Swelling of starch granules are normally studied during gelatinisation of starch occurring when starch is heated in the excess of water (Hoover 2001; Jenkins & Donald 1998; Singh & Kaur 2004). However, when starch granules were added to water low rate swelling is expected due to water binding even at lower temperatures. The early volume increase coincided with an increase in OUR indicating significant microbial growth (figure 1). This first microbial colonization and growth phase, is indicated by a dashed line at 4 days in figure 1. Earlier research has shown an initial fast adsorption of starch to activated sludge flocs at low F/M-

18

302 ratios (Ciggin et al. 2013; Karahan et al. 2006; Martins et al. 2011). However, microscopy

303 (figure 4) did not show any flocculation of starch particles to activated sludge flocs in the

304 early phases of this experiment with a high F/M-ratio. Hence, our results indicate a combined

305 starch granule swelling and biomass growth effect on observed size distribution, and not a

306 flocculation effect. Due to the low initial biomass content, absolute increase in biomass over

307 the first days will be small even at maximum growth rate. After initial volume increase,

308 particle number continued to increase until day 20 (figure 2), this number increase was likely

309 the combined effect of biomass growth and particle breakup.

310 After approximately 40 days, particle distribution shifted away from initial starch granule

311 distribution to smaller particle sizes (figure 3), surface area to volume ratio was constant

312 (figure 2) and only flocculated biomass was observed (figure 4). This coincided with a shift in

313 OUR from a stable high OUR to a linearly decreasing OUR over time indicated by dashed

314 lines (figure 1). HMW polymeric substrate was measured in the bulk liquid at high levels at

315 the time of this shift in OUR (figure 5). The system had at this point shifted from a starch

316 particle, to a biomass particle dominated system, and the substrate shifted from microscale

317 particle to dissolved polymers with high molar mass (figure 6). Hence, the stable OUR phase

318 (between day 4 and 36) of the experiment was a period dominated by particle degradation,

319 while the steadily decreasing OUR phase (after day 36) was a phase dominated by HMW

320 polymeric intermediate degradation and biomass decay (figure 2).

321 An OUR peak of about 2 mg L^{-1} h^{-1} was measured in this experiment during the particle

322 degradation phase (figure 1). This is 25-100 times lower than literature data of starch

323 degradation in sequencing batch reactors (Ciggin et al. 2013; Karahan et al. 2006), and 3-4

324 times lower than OUR rates measured on egg white particles in batch reactors (Dimock &

325 Morgenroth 2006) and settleable wastewater fractions (Ginestet et al. 2002). This difference

326   can be explained by an initially higher F/M-ratio used in this experiment compared to the

327   other studies.

What is the mechanism and dynamics of starch particle degradation?

329   Starch particles were colonized by microbial biomass (figure 4), supporting colonization of

330   particles as mechanism for particle degradation (Ravndal et al. 2015). All starch particles

331   were not immediately colonized, or biomass intermittently detached as starch particles free of

332   biomass were observed also at later stages in the experiment. In addition to particle

333   colonization, particle cracking was observed by microscopy (figure 4), and starch granules

334   became more heterogeneous over time. Cracking of particles could be a combined effect of

335   free extracellular enzymatic activity, hydration and physical-chemical fragmentation.

336   Extracellular enzymes are able to attack brittle zones of the starch granules and lead to pit and

337   pore formation on the particle surface (Gallant et al. 1992; Robyt 2009; Tang et al. 2006).

338   This results in an increased surface area. Finally, particle breakup leading to formation of

339   smaller and more heterogeneous particles was microscopically observed (figure 4). This was

340   supported by total particle volume and surface area measurements (figure 2), and by changes

341   in PSD (figure 3). After the early volume increase, surface area continued to increase while

342   volume started to decrease. This lead to an increasing surface area to volume ratio over time.

343   If degradation followed the SPM, surface area should gradually decrease throughout the

344   particle degradation phase. On the other hand, in the PBM particle breakup lead to an early

345   increase in surface area when the rate of particle breakup is larger than removal rate of

346   particulate substrate due to further biodegradation (Dimock & Morgenroth 2006). Our results

347   show an increase in surface area simultaneous as the overall volume of particles decrease

348   (figure 2), hence, degradation follow the PBM and not the SPM. Dimock and Morgenroth

349   (2006) proposed particle breakup as the main mechanism, but also hypothesized that

350   increased particle porosity and increase in particle colonization could explain the kinetics of

351 the PBM model. Based on our results, all three factors seem to contribute to particle

352 degradation.

353 Glucose, maltose, larger oligomers and polymers were detected in the bulk liquid, and it is

354 hypothesised that these are intermediates formed during particle hydrolysis (figure 5).

355 Maltose has earlier been detected as primary end-product for hydrolysis of starch by activated

356 sludge (Karahan et al. 2006; Ubukata 1999), while we detected both glucose and maltose

357 when batch tests was inoculated with activated sludge. Release of intermediates to the bulk

358 liquid in this experiment confirms earlier studies showing release of dissolved organic carbon

359 to the bulk liquid during activated sludge starch degradation (Karahan et al. 2006; Ubukata

360 1999). Contrary to our results, Martins et al. (2011) did not observe bulk phase intermediates

361 during starch degradation in activated sludge sequencing batch reactors. If intermediates are

362 not detected, they can be assumed to be consumed close to their production site (Martins et al.

363 2011). In systems with a low F/M-ratio, such as the study by Martins et al. (2011) it is also

364 possible that diffusion into the bulk liquid is limited due to particulate substrate being fully

365 surrounded by biomass. However, our results at an initially high F/M-ratio and several other

366 studies with a low F/M-ratio (Confer & Logan 1997; Karahan et al. 2006; Ubukata 1999)

367 report intermediate release to the bulk liquid during starch degradation. Thus, it is important

368 to consider also degradation mechanism and dynamics of polymeric intermediates when

369 modelling degradation of starch, and potentially any substrate particles. Most existing models,

370 however, do not consider a soluble polymeric intermediate fraction (Morgenroth et al. 2002).

371 Another explanation of polymers being detected in the bulk liquid during the experiment is

372 release of soluble microbial products (SMP). SMPs are defined as DOM released to the bulk

373 liquid due to substrate metabolism/biomass growth and biomass decay (Barker & Stuckey

374 1999). Size distribution of SMP identified in earlier research and summarised in Barker and

375 Stuckey (1999) show that SMP have a wide, but lower molecular weight distribution than

21

376 reported here. The analysis method used for molecular weight measurements were not

377 specific for starch intermediates, hence SMP were included in the total polymer data.

378 However, due to the large size of HMW polymers, we conclude that the majority of polymers

379 measured in the bulk liquid were in fact intermediates produced outside the bacterial cell due

380 to starch degradation.

381 Based on observed intermediate and particle dynamics, we propose a conceptual model

382 including intermediate dynamics for the extracellular enzymatic degradation of starch (figure

383 7a). Upon microbial colonization of starch particles, hydrolytic extracellular enzymes are

384 released in the contact zone between bacteria and starch particles. Polymeric, oligomeric and

385 monomeric intermediates formed during particle degradation may diffuse into the bulk liquid.

386 Polymeric and oligomeric intermediates are subsequently depolymerised into easily

387 biodegradable oligomers and monomers that are readily taken up by growing microbial cells.

388 All size intermediates may be expected, however based on our results and for

389 conceptualization, polymeric intermediates are grouped into HMW, MMW and LMW

390 fractions.

391
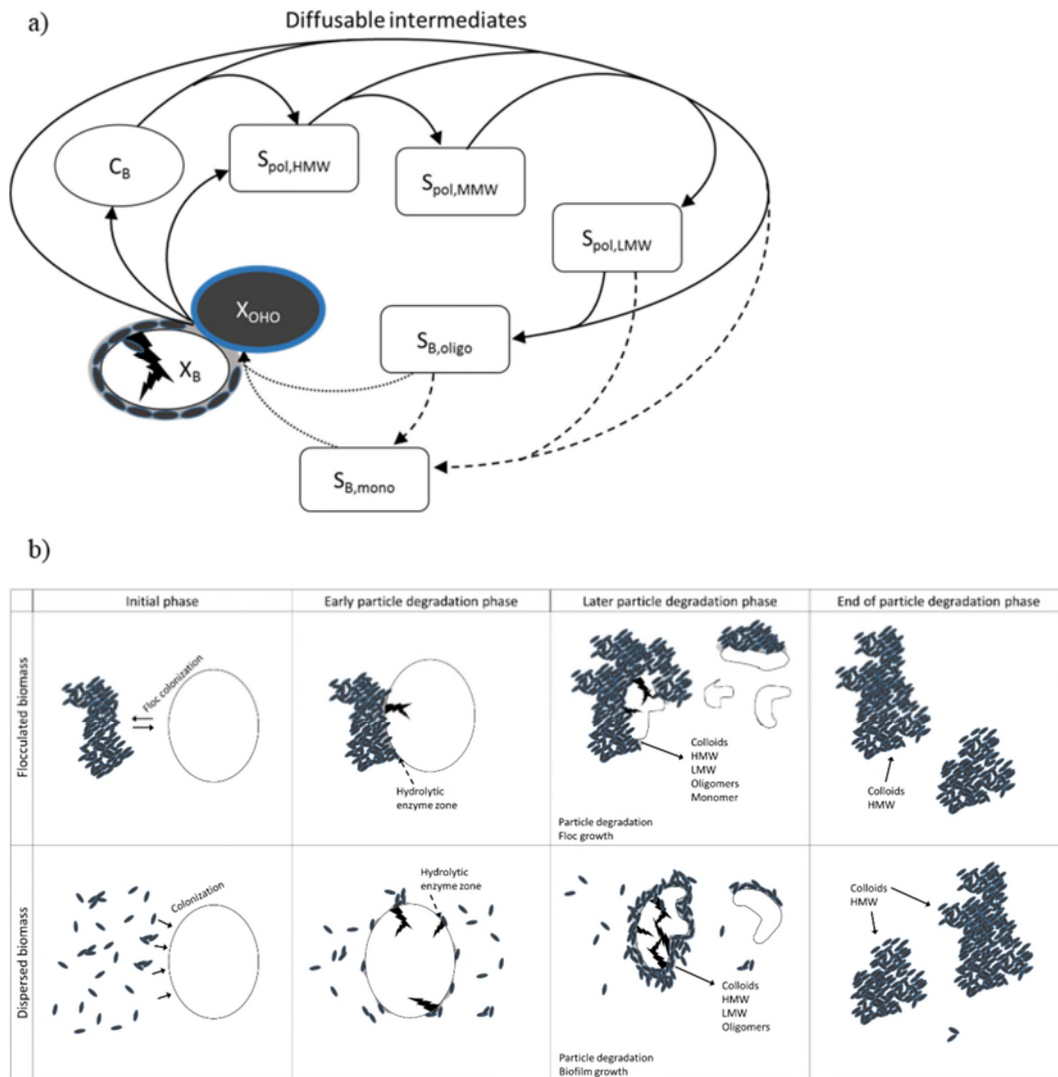
Figure 7: a) Conceptual COD flow model of starch (X_B) depolymerisation. The model assumes a colonized

starch surface to be the hotspot of extracellular hydrolytic activity, whereby exo- (dashed lines) and

endoenzymatic (solid lines) degradation of particulate (oval boxes) and dissolved polymers (Square boxes) leads

to diffusible intermediates that undergo further depolymerisation to oligo ($S_{B,oligo}$) and monomeric ($S_{B,mono}$) easily

biodegradable substrates that are readily taken up by growing cells (X_{OHO}) (dotted lines). The largest

degradation product of starch are colloids (C_B). Polymeric intermediates are separated in HMW ($S_{pol,HMW}$),

MMW ($S_{pol,MMW}$) and LMW ($S_{pol,LMW}$). New and existing model variables are implemented with standardised

notation proposed by Corominas et al. (2010). b) Conceptual model of biomass substrate interactions during

particle degradation with flocculated and dispersed biomass. Four different phases of degradation are

differentiated.

402

403   Monomers and oligomers are expected to be released during enzymatic degradation of starch

404   (Robyt 2009). In our study, monomers and oligomers formed during depolymerisation were

405   detected in the bulk liquid only in the beginning of the experiment (figure 5), indicating

406   monomer and oligomer formation and diffusion into the bulk liquid to be higher than uptake

407   rate at that stage. Later, these were no longer measured in the bulk liquid, indicating limited

408   diffusion into the bulk liquid due to starch particles being fully colonized by bacteria.

409   Alternatively, this can also be explained by uptake of released easily biodegradable substrate

410   in the bulk liquid under high suspended biomass concentrations following suspended growth

411   or detachment of biomass from the particles.

412   By qualitative comparison to our data, intermediate polymers in the form of amylopectin,

413   amylose and polymeric degradation products of the two were released to the bulk liquid

414   (figure 5 and 6). LMW polymers were released at high concentrations early in the experiment,

415   suggesting these to be formed directly from particle degradation. The LMW polymeric

416   fraction include several of the known products of enzymatic degradation of starch (Robyt

417   2009). When starch particles no longer were detected in the bulk liquid, HMW polymer

418   concentration was still increasing, indicating the presence of a colloidal fraction in between

419   measured HMW polymer and particle fraction.

420   Low concentrations of MMW polymers were detected in the bulk liquid (figure 5), in addition

421   the measured molar mass of HMW polymers were very high (figure 6). This was either due to

422   difference in hydrolysis rate between different fractions, or it means that not all intermediate

423   polymer sizes were formed. Earlier research has shown that hydrolysis rate increase as

424   molecular weight decreases (Kommedal et al. 2006), potentially leading to faster removal

425   than production of smaller polymer sizes. However, this can also be explained by a non

426   random degradation pattern of starch and larger HMW polymers by extracellular enzymes.

427   Others have shown that the enzymes degrading starch do not have a random degradation

428 pattern, but enzymes from different organisms will produce different products in variable

429 amounts (Robyt 2009). Most enzymes will produce oligomers as end-products, while larger

430 polymers would be a minor degradation product. This can be illustrated by the action of

431 bacterial β-amylases, which act towards amylopectin and form about 50 % maltose and 50 %

432 HMW polymers (Robyt 2009). β-amylases cannot pass α-1,6-branching points, hence HMW

433 polymers are formed when the enzyme reaches a branching point. Another starch acting

434 enzyme, α-amylases, normally lead to production of oligomers (Robyt 2009), and larger

435 polymers would be minor degradation product formed when the overall polymer size are

436 reduced. MMW polymers were only detected in the bulk liquid after HMW polymer

437 concentration increased. This indicates that MMW polymers were a degradation product from

438 HMW polymer hydrolysis, and not from starch hydrolysis. This support the hypothesis that

439 this is a minor degradation product formed as overall polymer size decreases, and not a major

440 product of enzymatic degradation of starch. Hence, even though hydrolysis rate increase with

441 decreasing polymer size, size distribution of polymeric intermediates, and timing of the

442 different size classes indicates that all potential intermediate sizes were not formed to the

443 same amount.

444 Protozoa have been shown to be able to directly feed on starch (de Kreuk et al. 2010). In this

445 experiment protozoa was seen by microscopy, but mainly late in the experiment (after 30

446 days). They therefore did not contribute to significant starch degradation, but probably

447 affected biomass decay rates.

448 Can initial biomass composition have an effect on mechanism and observed dynamics

449 of particle degradation?

450 Overall degradation was the same with little difference in accumulated oxygen consumption

451 over 97 days for flocculated and dispersed biomass. The most distinctive difference observed

25

452 was detection of glucose in the bulk liquid only in batch tests fed with flocculated biomass

453 (figure 5). Maltose was detected in the bulk liquid of both systems(figure 5). This could be

454 due to a higher exo-enzymatic activity in flocculated biomass tests leading to a higher

455 formation of glucose, or a difference in transport of glucose between flocculated and

456 dispersed biomass tests. Sonication was performed on a sub-volume of collected activated

457 sludge, hence the same microbes should be present in both tests and there should not be a

458 genotypic exo-enzymatic difference. Therefore, a more likely explanation is that transport of

459 glucose was different in dispersed and flocculated activated sludge batch test.

460 The differences in transport regimes and particle biomass interactions between the two

461 systems are presented in a proposed conceptual model (figure 7b). In flocculated biomass

462 tests, colonization can be assumed to be floc-based, and the initial high F/M-ratio means that

463 the substrate was partially colonized. On the other hand, the dispersed biomass allow for the

464 entire substrate particles to adsorb bacteria, and form an initial thin biofilm covering the entire

465 surface of the substrate. After initial colonization, the colonized surface would be e a hot-spot

466 for extracellular enzyme activity. However, truly extracellular enzymes would also be free to

467 diffuse to uncovered areas of the particle surface. Similarly, glucose produced on the starch

468 particle surface in the early particle degradation phase (figure 7b), would diffuse into the bulk

469 liquid for the partially covered substrate in both systems. However, the diffusion distance for

470 glucose back into the flocculated biomass is longer compared to the short diffusion distance

471 required by homogenously distributed single cells (Stewart 2003). Hence, glucose accumulate

472 in the bulk liquid due to diffusion limitations for the flocculated system. On the other hand,

473 for the dispersed system, glucose are consumed fast by free cells and do not accumulate. In

474 the later stages, a thin biofilm can fully cover the entire starch particle surface in the dispersed

475 system and glucose produced on the surface would be directly consumed, and not diffuse into

476 the bulk liquid. Hence, for the dispersed system the combination of biofilm formation and

477   non-limited transport explained why glucose did not accumulate. For larger intermediates,

478   there is no difference between the two systems, an aspect explained by diffusion coefficients

479   decreasing with increasing molecular weight leading to accumulation in both systems.

480   PSD shifted towards smaller diameters at a slower rate in the dispersed biomass tests,

481   compared to the flocculated biomass system (figure 3 and figure 2b). This can be explained

482   by either flocculation of the dispersed biomass and a difference in particle break-up between

483   the two systems. Due to a very low F/M-ratio, the effect of biomass flocculation would be

484   minimal. Hence, the difference in PSD, indicate that for flocculated biomass, particles were

485   breaking up into smaller particles at a faster rate than for dispersed biomass tests. Hence,

486   increased porosity and colonization played a larger role for dispersed biomass, while particle

487   breakup was more important with flocculated biomass. This can be explained by the proposed

488   substrate and biomass interaction model (figure 7b). Formation of a colonization biofilm over

489   a larger surface area by dispersed biomass, lead to extracellular enzymes attacking a larger

490   area of the particle. Enzyme attack lead to pit and pore formation on the particle surface

491   (Gallant et al. 1992; Robyt 2009; Tang et al. 2006), and could explain particle cracking seen

492   by microscopy. Pit and pore formation on the surface of the particles would again lead to

493   increased particle porosity.

494   Towards the end of the particle degradation phase, the biomass will converge in the two

495   systems as illustrated in the conceptual biomass model (figure 7b). This is supported by a

496   comparable surface area to volume ratio (figure 2), by PSDs (figure 3a and 3b) and by

497   microscopy pictures (figure 4). Biomass particles measured in the system after the particle

498   degradation phase has a mean spherical particle diameter of 10 µm. This show that particulate

499   substrate lead to floc-formation of the biomass due to colonization. Hence, during the

500   degradation phase dominated by HMW polymers as substrate, the difference of a flocculated

501   and dispersed biomass system cannot be evaluated.

The results and conclusions gained in this work have implications for the way we understand particle degradation in bioprocesses. For the general case, intermediates form during particle and polymer degradation, and the biomass transport regime could allow for considerable intermediate accumulation in the bulk phase. When adequate, models used for particulate/polymeric slow biodegradable analysis should reflect this aspect of the system, as indicated by the conceptual models proposed herein. For systems with short hydraulic retention times, like biofilm and granulated biomass processes, significant fractions of COD would be lost to effluents reducing treatment performance and bioproduct yields. This is relevant for water and wastewater treatment systems, as well as bioenergy and biofuels processes based on particulate substrates.

Conclusions

- All intermediate polymer sizes are not formed to the same extent during starch particle degradation indicating non-random enzymatic degradation, either low or ultra high molecular weigh polymers are preferred.

- During starch particle degradation, intermediate dynamics depend on the biomass structure. In a floc-based system, diffusion limitations allow glucose to accumulate in the system. This is a generic effect of bioaggregates.

- The combination of particle colonization, increased particle porosity and particle breakup led to increased substrate availability during particle degradation. Particle breakup was more important for flocculated biomass, while particle colonization and increased particle porosity was more important for dispersed biomass.

References

Balch, W.E., Fox, G., Magrum, L., Woese, C., Wolfe, R. 1979. Methanogens: reevaluation of a unique biological group. *Microbiological reviews*, **43**(2), 260.

Ball, S., Guan, H.P., James, M., Myers, A., Keeling, P., Mouille, G., Buleon, A., Colonna, P., Preiss, J. 1996. From glycogen to amylopectin: A model for the biogenesis of the plant starch granule. *Cell*, **86**(3), 349-352.

Barker, D.J., Stuckey, D.C. 1999. A review of soluble microbial products (SMP) in wastewater treatment systems. *Water Research*, **33**(14), 3063-3082.

Batstone, D.J., Keller, J., Angelidaki, I., Kalyuzhnyi, S., Pavlostathis, S., Rozzi, A., Sanders, W., Siegrist, H., Vavilin, V. 2002. The IWA anaerobic digestion model no 1 (ADM1). *Water Science and Technology*, **45**(10), 65-73.

Cheong, K.L., Wu, D.T., Zhao, J., Li, S.P. 2015. A rapid and accurate method for the quantitative estimation of natural polysaccharides and their fractions using high performance size exclusion chromatography coupled with multi-angle laser light scattering and refractive index detector. *Journal of Chromatography A*, **1400**, 98-106.

Ciggin, A.S., Insel, G., Majone, M., Orhon, D. 2013. Model evaluation of starch utilization by acclimated biomass with different culture history under pulse and continuous feeding. *Bioresource Technology*, **138**, 163-171.

Confer, D.R., Logan, B.E. 1997. Molecular weight distribution of hydrolysis products during the biodegradation of model macromolecules in suspended and biofilm cultures .2. Dextran and dextrin. *Water Research*, **31**, 2137-2145.

Corominas, L., Rieger, L., Takács, I., Ekama, G., Hauduc, H., Vanrolleghem, P.A., Oehmen, A., Gernaey, K.V., van Loosdrecht, M.C.M., Comeau, Y. 2010. New framework for standardized notation in wastewater treatment modelling. *Water Science and Technology*, **61**, 841-857.

de Kreuk, M.K., Kishida, N., Tsuneda, S., van Loosdrecht, M.C.M. 2010. Behavior of polymeric substrates in an aerobic granular sludge system. *Water Research*, **44**, 5929-5938.

Dimock, R., Morgenroth, E. 2006. The influence of particle size on microbial hydrolysis of protein particles in activated sludge. *Water Research*, **40**, 2064-2074.

Dona, A.C., Pages, G., Gilbert, R.G., Kuchel, P.W. 2010. Digestion of starch: In vivo and in vitro kinetic models used to characterise oligosaccharide or glucose release. *Carbohydrate Polymers*, **80**(3), 599-617.

Feitkenhauer, H., Meyer, U. 2002. Anaerobic digestion of alcohol sulfate (anionic surfactant) rich wastewater - batch experiments. Part 1: influence of the surfactant concentration. *Bioresource Technology*, **82**(2), 115-121.

Gallant, D., Bouchet, B., Buleon, A., Perez, S. 1992. Physical characteristics of starch granules and susceptibility to enzymatic degradation. *European journal of clinical nutrition*, **46**, S3-16.

Ginestet, P., Maisonnier, A., Sperandio, M. 2002. Wastewater COD characterization: biodegradability of physico-chemical fractions. *Water Science and Technology*, **45**(6), 89-97.

Goel, R., Mino, T., Satoh, H., Matsuo, T. 1998. Enzyme activities under anaerobic and aerobic conditions inactivated sludge sequencing batch reactor. *Water Research*, **32**, 2081-2088.

Henze, M., Gujer, W., Mino, T., van Loosdrecht, M. 2000. *Activated sludge models ASM1, ASM2, ASM2d and ASM3*. IWA Publishing, London.

Hoover, R. 2001. Composition, molecular structure, and physicochemical properties of tuber and root starches: a review. *Carbohydrate Polymers*, **45**(3), 253-267.

Jenkins, P.J., Donald, A.M. 1998. Gelatinisation of starch: a combined SAXS/WAXS/DSC and SANS study. *Carbohydrate Research*, **308**(1–2), 133-147.

Karahan, O., Martins, A., Orhon, D., van Loosdrecht, M.C.M. 2006. Experimental evaluation of starch utilization mechanism by activated sludge. *Biotechnology and Bioengineering*, **93**(5), 964-970.

Kommedal, R. 2003. Degradation of polymeric and particulate organic carbon in biofilms, Norwegian University of Science and Technology, Trondheim, pp. 168.

Kommedal, R., Milferstedt, K., Bakke, R., Morgenroth, E. 2006. Effects of initial molecular weight on removal rate of dextran in biofilms. *Water Research*, **40**, 1795-1804.

Levine, A.D., Tchobanoglous, G., Asano, T. 1991. Size distributions of particulate contaminants in wastewater and their impact on treatability. *Water Research*, **25**(8), 911-922.

Martins, A.M.P., Karahan, O., van Loosdrecht, M.C.M. 2011. Effect of polymeric substrate on sludge settleability. *Water Research*, **45**(1), 263-273.

Morgenroth, E., Kommedal, R., Harremoes, P. 2002. Processes and modeling of hydrolysis of particulate organic matter in aerobic wastewater treatment - a review. *Water Science and Technology*, **45**, 25-40.

Oates, C.G. 1997. Towards an understanding of starch granule structure and hydrolysis. *Trends in Food Science & Technology*, **8**(11), 375-382.

Ravndal, K.T., Künzle, R., Derlon, N., Morgenroth, E. 2015. On-site treatment of used wash-water using biologically activated membrane bioreactors operated at different solids retention times. *Journal of Water Sanitation and Hygiene for Development*, **5**(4), 544-552.

Robyt, J.F. 2009. Enzymes and their action on starch. in: *Starch: Chemistry and technology*, J. BeMiller, R. Whistler (Eds.). 3rd edn, Academic Press, Amsterdam, pp. 237-292.

Sanders, W.T.M., Geerink, M., Zeeman, G., Lettinga, G. 2000. Anaerobic hydrolysis kinetics of particulate substrates. *Water Science and Technology*, **41**(3), 17-24.

Singh, N., Kaur, L. 2004. Morphological, thermal, rheological and retrogradation properties of potato starch fractions varying in granule size. *Journal of the Science of Food and Agriculture*, **84**(10), 1241-1252.

Stewart, P.S. 2003. Diffusion in biofilms. *Journal of bacteriology*, **185**(5), 1485-1491.

Sun, H., Zhao, P., Ge, X., Xia, Y., Hao, Z., Liu, J., Peng, M. 2010. Recent advances in microbial raw starch degrading enzymes. *Applied Biochemistry and Biotechnology*, **160**(4), 988-1003.

Tang, H., Mitsunaga, T., Kawamura, Y. 2006. Molecular arrangement in blocklets and starch granule architecture. *Carbohydrate Polymers*, **63**(4), 555-560.

613   Ubukata, Y. 1999. Kinetics and fundamental mechanisms of starch removal by activated
614   sludge: Hydrolysis of starch to maltose and maltotriose is the rate-determining step.
615   *Water Science and Technology*, **40**(1), 61-68.

616   Vavilin, V.A., Fernandez, B., Palatsi, J., Flotats, X. 2008. Hydrolysis kinetics in anaerobic
617   degradation of particulate organic material: An overview. *Waste Management*, **28**(6),
618   939-951.

619   Vavilin, V.A., Rytov, S.V., Lokshina, L.Y. 1996. A description of hydrolysis kinetics in
620   anaerobic degradation of particulate organic matter. *Bioresource Technology*, **56**(2-3),
621   229-237.

622   White, D., Drummond, J., Fuqua, C. 2012. *The physiology and biochemistry of prokaryotes.*
623   *4th ed*. Oxford university press, Oxford.

624   Wyatt, P.J. 1993. Light scattering and the absolute characterization of macromolecules.
625   *Analytica Chimica Acta*, **272**(1), 1-40.

626   Xia, Y., Kong, Y.H., Nielsen, P.H. 2008. In situ detection of starch-hydrolyzing
627   microorganisms in activated sludge. *Fems Microbiology Ecology*, **66**(2), 462-471.

628